Inorganic Chemistry

Article

pubs.acs.org/IC

Metal Atom Dynamics in Superbulky Metallocenes: A Comparison of $(Cp^{BIG})_2Sn$ and $(Cp^{BIG})_2Eu$

Sjoerd Harder,*[,†] Dominik Naglav,[‡] Peter Schwerdtfeger,[§] Israel Nowik,[⊥] and Rolfe H. Herber*[,⊥]

[†]Inorganic and Organometallic Chemistry, University Erlangen-Nürnberg, Egerlandstrasse 1, 91058 Erlangen, Germany

[‡]Anorganische Chemie, Universität Duisburg-Essen, Universitätsstrasse 5, 45117 Essen, Germany

[§]Centre for Theoretical and Chemistry and Physics (CTCP), New Zealand Institute for Advanced Stsudy (NZIAS), Massey University (Albany Campus), Private Bag 102904, North Shore MSC, Auckland, New Zealand

[⊥]Racah Institute for Physics, The Hebrew University, 91904 Jerusalem, Israel

ABSTRACT: $Cp^{BIG}{}_2Sn$ (Cp^{BIG} = (4-*n*-Bu-$C_6H_4)_5$cyclopentadienyl), prepared by reaction of 2 equiv of $Cp^{BIG}Na$ with $SnCl_2$, crystallized isomorphous to other known metallocenes with this ligand (Ca, Sr, Ba, Sm, Eu, Yb). Similarly, it shows perfect linearity, C−H···C(π) bonding between the Cp^{BIG} rings and out-of-plane bending of the aryl substituents toward the metal. Whereas all other $Cp^{BIG}{}_2M$ complexes show large disorder in the metal position, the Sn atom in $Cp^{BIG}{}_2Sn$ is perfectly ordered. In contrast, ^{119}Sn and ^{151}Eu Mößbauer investigations on the corresponding $Cp^{BIG}{}_2M$ metallocenes show that Sn(II) is more dynamic and loosely bound than Eu(II). The large displacement factors in the group 2 and especially in the lanthanide(II) metallocenes $Cp^{BIG}{}_2M$ can be explained by static metal disorder in a plane parallel to the Cp^{BIG} rings. Despite parallel Cp^{BIG} rings, these metallocenes have a nonlinear Cp_{center}−M−Cp_{center} geometry. This is explained by an ionic model in which metal atoms are polarized by the negatively charged Cp rings. The extent of nonlinearity is in line with trends found in M^{2+} ion polarizabilities. The range of known calculated dipole polarizabilities at the Douglas−Kroll CCSD(T) level was extended with values (atomic units) for Sn^{2+} 15.35, $Sm^{2+}(4f^6\ ^7F)$ 9.82, $Eu^{2+}(4f^7\ ^8S)$ 8.99, and $Yb^{2+}(4f^{14}\ ^1S)$ 6.55. This polarizability model cannot be applied to predominantly covalently bound $Cp^{BIG}{}_2Sn$, which shows a perfectly ordered structure. The bent geometry of $Cp^*{}_2Sn$ should therefore not be explained by metal polarizability but is due to van der Waals Cp*···Cp* attraction and (to some extent) to a small *p*-character component in the Sn lone pair.

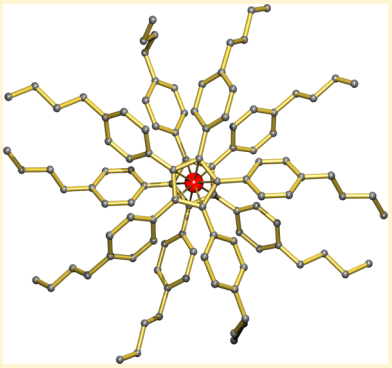

INTRODUCTION

The structures of the heavier alkaline-earth metal sandwich complexes $Cp^*{}_2M$ (**1**; Cp = cylclopentadienyl, M = Ca, Sr, and Ba) and the divalent lanthanide(II) metallocenes (M = Yb, Eu, Sm) have been the subject of a large number of research reports.[1−14] This is due to their unusual bent geometries, which are not only present in the solid state but also prevalent in the gas phase. Bending of these sandwich complexes increases with metal size, and a linear relationship between bending angle α (defined in Formula 1) and the Cp-metal distance is observed.[8]

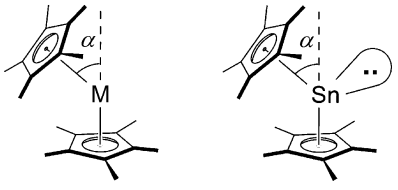

1 2

This bending is not fully understandable in the light of VSEPR theory or on basis of electrostatic considerations. A long discussion in the literature culminated in two major explanations for this phenomenon. Polarization of the core electrons of these heavier metals have been made responsible: the nonlinear arrangement of negatively charged Cp rings induces a dipole moment on the metal that results in increased ligand−metal attraction (Scheme 1a). Another theory underscores the importance of weak but attractive van der Waals

Scheme 1

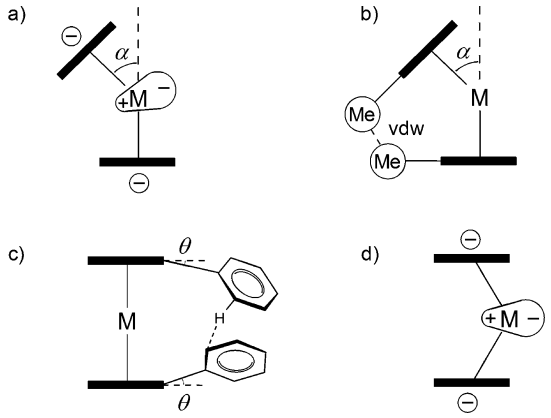

Received: November 15, 2013
Published: February 5, 2014

   dx.doi.org/10.1021/ic4028546 | *Inorg. Chem.* 2014, 53, 2188−2194

Table 1. Comparison of Geometrical Parameters for Deca-arylmetallocenes (Distances in Å and Angles in Degrees)

	M^{2+} radius[a]	av. M−C	M−Cp_{center}	C−H···C	θ^b	α^c M^{2+}	ref (α)	U_{eq}
$(Ph_5Cp)_2Sn$[19]	0.93	2.691(7)	2.401(3)	2.68[160]	1.2(4)	15.35	this Work	
$Cp^{BIG}{}_2Sn$	0.93	2.693(2)	2.4030(9)	2.65[155]	1.24(1)	15.35	this Work	0.029
$Cp^{BIG}{}_2Ca$[26]	1.00	2.651(1)	2.3561(4)	2.58[155]	1.21(6)	3.26	34	0.034
$Cp^{BIG}{}_2Sr$[25]	1.18	2.790(2)	2.513(1)	2.69[152]	3.4(2)	5.79	34	0.057
$Cp^{BIG}{}_2Ba$[25]	1.35	2.929(2)	2.667(1)	2.81[149]	5.3(2)	10.49	34	0.056
$Cp^{BIG}{}_2Sm$[26]	1.22	2.782(2)	2.505(2)	2.67[152]	3.5(1)	9.82	this Work	0.076
$Cp^{BIG}{}_2Eu$[27]	1.17	2.776(2)	2.497(2)	2.68[152]	3.1(2)	8.99	this Work	0.075
$Cp^{BIG}{}_2Yb$[26]	1.02	2.673(2)	2.382(1)	2.61[154]	1.4(1)	6.55	this Work	0.058

[a]Radii for 6-coordinate metal ions (for Sm 7-coordinate) taken from Shannon & Prewitt.[28] [b]Out-of-plane bending angle (see Scheme 1c). [c]Calculated dipole polarizabilities for the 2+ metal cations in atomic units at the DK-CCSD(T) level.

interactions between the Me substituents on neighboring Cp* ligands (Scheme 1b). Both arguments are in line with the observed correlation between bending and metal size. A similar situation is found for the group 2 fluorides, of which the bent structures have been investigated and analyzed extensively in the past by theoretical methods.[6,9]

In contrast to heavier group 2 metalllocenes, the bent structure of $Cp^*{}_2Sn$ (**2**) is intuitively explained by assuming a stereoactive sp^2 lone pair of electrons at the Sn(II) center. Hanusa et al., however, found strong structural similarities between group 2, lanthanide(II), and divalent group 4 metallocenes (Si, Sn, Pb). The late main-group metallocenes follow the same linear relationship between metal size and bending as observed for the early main-group metallocenes.[8] Although counterintuitive at first sight, Hanusa et al. proposed that bending of late main-group metallocenes might have the same origin as that of early main-group metallocenes. Indeed, Mößbauer studies show that a large part of the lone-pair electron density is in a symmetrical (nondirectional) orbital of mainly s and very little p character.[15] This is in line with the reactivity of stannocenes with electrophiles: intuitively Sn lone-pair nucleophilicity is expected, but cyclopentadienyl ring reactivity is found.[16] Thus, the lone pair in stannocenes is stereo and chemically inactive. Similar to early main-group metallocenes, bending can be rationalized by polarization and van der Waals arguments.

Increasing the steric bulk in these metallocenes generally leads to linearization of the bent structures.[17,18] Decaphenylstannocene represents the first perfectly linear metallocene of a late main-group metal.[19] This sandwich complex, however, is completely insoluble and could only be crystallized from a 200 °C solution in 1-methylnaphtalene.[20] This is a general characteristic of decaphenylmetallocenes.[21] Its complete insolubility in common organic solvents not only hinders crystallization but also prevents any solution characterization by NMR.

Compared to Cp*, the Ph_5Cp ligand offers a superb steric protection of the metal center but also shows a markedly different electronic influence. Whereas Cp* features electron-releasing Me substituents that hamper reduction of the metal center,[22] electron-withdrawing Ph groups strongly stabilize low-oxidation state metals as evidenced by less negative reduction potentials.[23] To accelerate investigations on the chemistry of this unique ligand, we used an alkyl-substituted variant, $(4\text{-}n\text{-Bu-}C_6H_4)_5Cp$ (abbreviated Cp^{BIG}), which produces metallocenes that are even highly soluble in alkanes.[24,25] At first sight, crystal structures with the metals Ca,[26] Sr,[25] Ba[25] Yb,[26] Sm,[26] and Eu[27] show perfectly linear centrosymmetric metallocenes. Contrary to the expectation that Cp^{BIG} ligands repel each other, it was found that these ligands attract each other: all metallocenes show 10 short C−H···C interactions in a merry-go-round arrangement, and aryl groups are bent out-of-plane toward the metal center (Scheme 1c). Most interesting is the observation that the metals in the crystal structure refinement show large thermal displacement factors in a plane parallel to the Cp rings. This disorder increases with metal size and shows that, despite parallel Cp rings, also these metallocenes have nonlinear Cp_{center}−M−Cp_{center} geometries (Scheme 1d). This is likely due to polarization of the metal core by negatively charged Cp ligands, which leads to additional metal−Cp attraction. This Work deals with a comparison of the crystal structures and metal dynamics, as deduced by Mößbauer investigations, of the europocene $Cp^{BIG}{}_2Eu$ and the stannocene $Cp^{BIG}{}_2Sn$.

RESULTS AND DISCUSSION

The stannocene $Cp^{BIG}{}_2Sn$ was prepared by reaction of 2 equiv of $Cp^{BIG}Na$ with $SnCl_2$. Its high solubility in alkanes prevented isolation in high yield, and crystalline pure material was obtained in 37% yield. However, the high solubility also enables acquisition of solution NMR data. The ^{119}Sn NMR spectrum shows a signal at −2160 ppm, which is close to the −2200/−2230 ppm range found in the ^{119}Sn-CPMAS NMR spectrum for insoluble $(Ph_5Cp)_2Sn$.[21] The range of signals found in the solid-state NMR spectrum of $(Ph_5Cp)_2Sn$ is likely due to the presence of metallocenes with slightly different bending angles at Sn. The very low chemical shift, that is, high shielding, is consistent with that found in other stannocenes.[21]

Like all other metallocenes with the Cp^{BIG} ligand, $Cp^{BIG}{}_2Sn$ crystallizes in the spacegroup $P\bar{1}$ with very similar cell parameter and half a molecule in the asymmetric unit. The stannocene is crystallographically centrosymmetric (the metal is situated on an inversion center). If one does not consider the *n*-Bu groups, a higher form of S_{10} symmetry can be observed, that is, both propeller-like penta-aryl Cp ligands display opposite chirality. The distances and other geometrical parameter are listed in Table 1, which for comparison also contains data of all other known $Cp^{BIG}{}_2M$ sandwich complexes.

The average Sn−C and Sn−Cp_{center} distances are in between those observed for $Cp^{BIG}{}_2Ca$ and $Cp^{BIG}{}_2Sr$. Therefore, the effective ionic radius for Sn(II) should be estimated at 1.05 Å (the ionic radius of 0.93 Å for Sn(II) in Table 1 relates to Shannon-Prewitt).[28b] Furthermore, $Cp^{BIG}{}_2Sn$ shows similar geometric characteristics as discussed for the sandwiches with M = Ca, Sr, Ba and those with Sm, Eu, Yb. The metallocenes show a C−H···C hydrogen bond network between aryl groups of opposing Cp^{BIG} ligands (Scheme 1c). The average C−H···C bond length and angle of these nonclassical hydrogen bonds

dx.doi.org/10.1021/ic4028546 | Inorg. Chem. 2014, 53, 2188−2194

both fit well between those for Cp^{BIG}_2Ca and Cp^{BIG}_2Sr. Also in Cp^{BIG}_2Sn attractive $Cp^{BIG}\cdots Cp^{BIG}$ interactions are present. This is indicated by the out-of-plane bending angle θ of the aryl groups (Scheme 1c), and its value fits between those of the calcocene and strontocene. Therefore, the linear relationship between this out-of-plane bending and the Cp^{BIG}–M distance is again confirmed. Notice that all values for Cp^{BIG}_2Sn are close to those for $(Ph_5Cp)_2Sn$, implying that *n*-Bu substitution only influences the solubility and not its structural properties. $Cp^{BIG}\cdots Cp^{BIG}$ attraction is therefore solely due to the ten nonclassical C–H···C hydrogen bonds and not to attractive interactions between the hydrophobic alkyl chains.

Despite similarities, a large discrepancy between the stannocene and the other Cp^{BIG}_2M structures (Ca, Sr, Ba, Sm, Eu, Yb) is found: whereas U_{eq} for the alkaline-earth and lanthanide metals is too large for what would be expected for a heavier atom (Table 1; cf. the average U_{eq} for the Cp ring carbons is 0.040), the U_{eq} for Sn of 0.029 is small and in the normal range for a heavy atom (See Figure 1 for comparison). At first sight, this suggests that the sandwiched alkaline-earth and lanthanide metals are more dynamic than the heavier group 14 metal Sn. The following detailed temperature-dependent ^{119}Sn Mößbauer study on Cp^{BIG}_2Sn, however, suggests a different discussion. The results of these investigations are compared to the ^{151}Eu Mößbauer study on the europocene.[27]

A sample of the yellow solid Cp^{BIG}_2Sn was transferred in an inert atmosphere glovebox to an O-ring sealed Perspex sample holder and immediately cooled to liquid nitrogen temperature prior to insertion into the precooled cryostat. The ^{119}Sn Mößbauer spectra at 90 K evidence two resonance absorptions, one at an isomer shift (IS) of 3.83(3) mm s^{-1} and the other at an IS of 0.15(3) mm s^{-1} (a representative spectrum is shown in Figure 2). The resonance at 3.83(3) mm s^{-1} is due to Sn(II), which usually shows resonances above 2.5 mm s^{-1}. The resonance at 0.15(3) mm s^{-1} is assigned to an Sn(IV) species, which generally absorb below 2.0 mm s^{-1}. The latter is likely a contamination with SnO_2, either formed in the synthetic procedure or by oxidative hydrolysis during sample transport. This adventitious oxidation of the Cp^{BIG} metallocenes was also noted for the europocene, which was contaminated with a significant amount of an Eu(III) species (presumably Eu_2O_3). Note that, because of the very high molecular weight of Cp^{BIG}_2Sn (MW = 1570.9), a 3 wt % contamination with SnO_2 (MW = 150.7) translates to a 24 mol % content of the oxide. However, the Sn(II) and Sn(IV) resonances are separated well enough to allow the analysis of the Sn(II) signal in more detail (Table 2).

The isomer shift of the Sn(II) resonance at 3.83(3) mm s^{-1} (90 K, relative to $BaSnO_3$ at room temperature) is quite high and clearly identifies the stannous oxidation state. The Sn(II) resonance has a line width of 0.87(15) mm s^{-1}, which is slightly larger than that observed with other single-line absorbers. The quadrupole splitting (QS) parameter is quite small: 0.51(3) mm s^{-1} at 93 K. These values compare well with the experimentally found IS and QS values for $(Ph_5Cp)_2Sn$ of 3.74 mm s^{-1} and 0.58 mm s^{-1}, respectively. Because of the asymmetry in the coordination sphere of most Sn(II) compounds caused by the lone pair,[15] the majority of Sn(II) organometallics evidence a large QS of 1.5–2.3 mm s^{-1}. Decaarylstannocene is, in contrast to the strongly bent Cp^*_2Sn, strictly linear and a special case. The rather high value for the IS and low value for the QS are consistent with a stereochemically inert pair in a 5s orbital with some mixing of $5d_z^2$ character.[29]

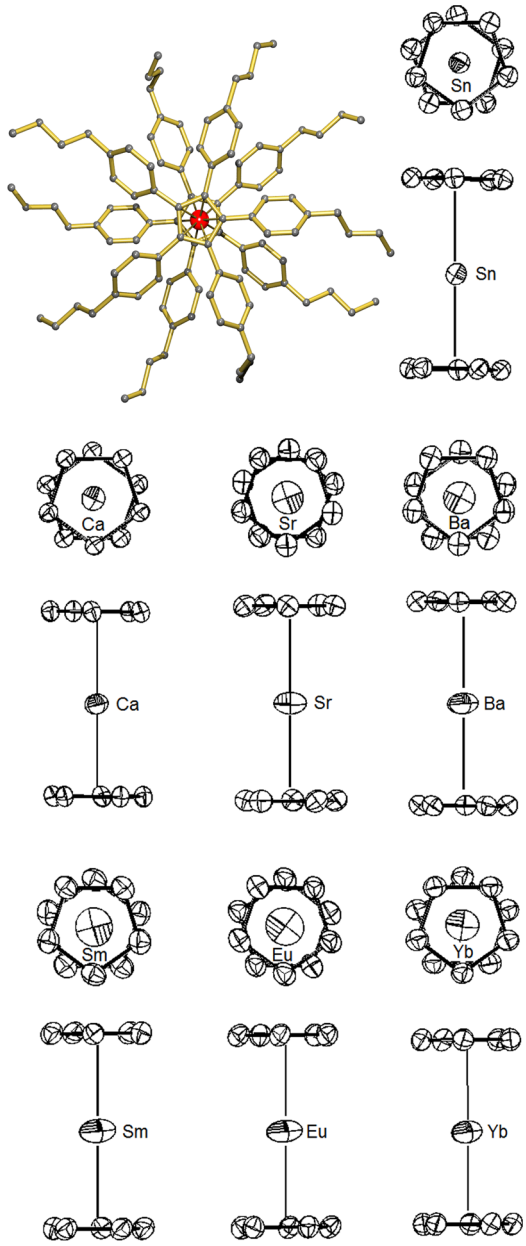

Figure 1. Crystal structure of Cp^{BIG}_2Sn with ORTEP representations of the Cp_2Sn fragment (50% probability ellipsoids) and comparison with Cp^{BIG}_2M crystal structures (M = Ca, Sr, Ba, Sm, Eu, and Yb).

Information on the dynamics of the Sn center can be obtained from temperature-dependent ^{119}Sn Mößbauer investigations. Because of the small value of the QS parameter and its temperature insensitivity, it is not possible to extract information concerning the anisotropy of the tin atom motion in Cp^{BIG}_2Sn from this parameter. Also the IS is not a sensitive function of temperature and shows upon heating from 90 to 193 K only a small decrease from 3.83(3) mm s^{-1} to 3.76(12) mm s^{-1}. The temperature dependence of the recoil-free fraction *f*, however, can be used to extract vibrational information on the metal atom. For an optically thin absorber, this parameter can be easily evaluated from the area under the resonance curve, and we determined *f* as function of temperature. Parameter *f* is related to the metal's dynamic behavior by the following. The area under the resonance peak for an optically thin absorber is given by $A = c \times n \times f$, where *c* is a proportionality constant, *n* is

dx.doi.org/10.1021/ic4028546 | Inorg. Chem. 2014, 53, 2188–2194

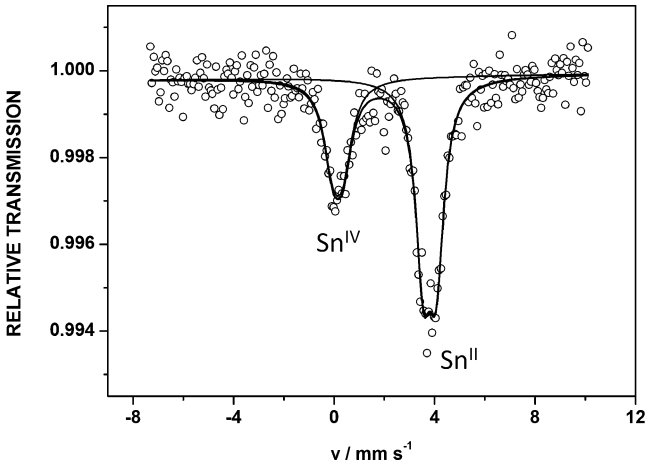

Figure 2. The ^{119}Sn Mößbauer spectrum of solid Cp^{BIG}_2Sn at 90 K.

Table 2. Summary of ^{119}Sn and ^{151}Eu Mößbauer Parameters

	Cp^{BIG}_2Sn	Cp^{BIG}_2Eu
$IS(90)_{M(II)}$ (mm s^{-1})	3.83(3)	−13.3(4)
$\Gamma(90)_{M(II)}$ (mm s^{-1})	0.87(15)	1.92
$QS(90)_{M(II)}$ (mm s^{-1})	0.52(4)	−3.96(5)
$-d(\ln A)/dT \times 10^{-3}$ K^{-1}	20.6(4)	10.9(4)
$F_{Möss}(203\ K)_{M(II)}$	4.17(6)	2.18(5)
$F_{X\text{-}ray}(203\ K)_{M(II)}$	4.17(2)	8.51(2)

the number of atoms in the optical path, and f is the recoil-free fraction equal to $\exp(-k^2\langle x_{ave}{}^2\rangle)$, in which k is the wave vector of the ^{119}Sn gamma ray and $\langle x_{ave}{}^2\rangle$ is the mean square amplitude of vibration of the Sn atoms in the sample at temperature T. The latter can be normalized making the assumption that $f \rightarrow 1$ as $T \rightarrow 0$ (ignoring the small contribution of the zero-point motion in the low-temperature limit). In the present case, the temperature dependence of ln f is well-fitted by a linear regression with a correlation coefficient of 0.994 for 10 data points (Figure 3). The numerical values are included in Table 3. The value of $-d(\ln A)/dT$ for Cp^{BIG}_2Sn is 20.6(4) × 10^{-3} K^{-1}, while the reported values for decaphenyl and pentaphenyl stannocene are 17.0 × 10^{-3} and 16.8 × 10^{-3} K^{-1}, respectively.[30] Clearly, the tin atom in Cp^{BIG}_2Sn is less tightly bound than that in the two other stannocenes.

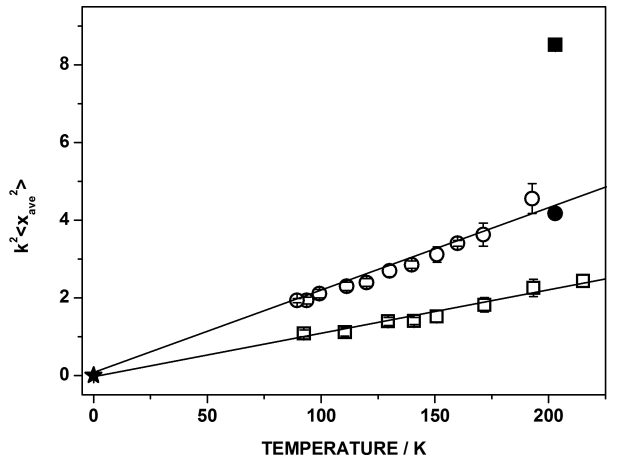

Figure 3. The $F_{Möss}(T)$ parameters ($k^2\langle x_{ave}{}^2\rangle$) for the Sn(II) site in Cp^{BIG}_2Sn (○) and the Eu(II) site in Cp^{BIG}_2Eu (□) as a function of temperature. The starred data point is the extrapolation of the Mössbauer data to T = 0 K, making the assumption that the zero-point motion in the high temperature regime is negligible. The filled circle (●) and square (■) are the $F_{X\text{-}ray}(203)$values calculated on the basis of the X-ray data for Sn and Eu, respectively (poor agreement for Eu is discussed in the text).

Table 3. Root Mean Square Amplitudes of Vibration for the Metal Atoms in Cp^{BIG}_2Sn and Cp^{BIG}_2Eu as a Function of Temperature

	Cp^{BIG}_2Sn		Cp^{BIG}_2Eu	
temperature (K)	$k^2\langle x_{ave}{}^2\rangle$	$\langle x^2\rangle^{0.5}$ Å	$k^2\langle x_{ave}{}^2\rangle$	$\langle x^2\rangle^{0.5}$ Å
100	2.28	0.125	1.07	0.095
150	3.41	0.153	1.60	0.116
200	4.55	0.176	2.14	0.134
250	5.68	0.197	2.67	0.150

As has been reported previously in connection with the dynamical behavior of metal atoms in organometallics,[31] the vibrational amplitudes derived from Mößbauer measurements can be compared to those extracted from single-crystal X-ray diffraction data. The appropriate parameter to consider is given by $F_{Möß}(T) = k^2\langle x_{ave}{}^2\rangle$, where k is the wavenumber of the Mößbauer gamma ray and $\langle x_{ave}{}^2\rangle$ is the mean square amplitude of vibration (msav) of the metal atom at temperature T. Similarly the $F_{X\text{-}ray}(T)$ parameter can be evaluated from the U_{ij} data of the X-ray diffraction experiment at a given temperature T. For Cp^{BIG}_2Sn the two values at 203 K (the temperature of the X-ray data) $F_{X\text{-}ray}(203\ K)$ = 4.17(2) and $F_{Möß}(203\ K)$ = 4.17(6) are in excellent agreement. The temperature dependence of $F_{Möß}$ and the single value for $F_{X\text{-}ray}$ are summarized graphically in Figure 3.

We recently published a similar temperature-dependent Mößbauer study for the europocene Cp^{BIG}_2Eu, which shows at 90 K a Mößbauer resonance at −13.3(4) mm s^{-1} for the Eu(II) site.[27] The hyperfine and derived parameters are also summarized in Table 2. The temperature dependence for $F_{Möß}$ over the range of 93−215 K and the single value for $F_{X\text{-}ray}$ are schematically shown in Figure 3. In the absence of further information it is worthwhile to focus on the F value for the Eu(II) site (2.18(5) at 203 K) only. Following the usual normalization procedure for the Mößbauer data it now becomes possible to compare the root mean square amplitude of vibration (rmsav) data for the Sn(II) site in the tin complex with that for the Eu(II) site in the present compound. This comparison at four temperatures, derived from the respective F values, is summarized in Table 3, from which it is noted that the rmsav for the Eu(II) site is smaller than it is for the Sn(II) site. Thus, Eu in Cp^{BIG}_2Eu is more tightly bound than Sn is bound in Cp^{BIG}_2Sn.

Of particular interest is a comparison of the $F_{Möß}(T)$ and $F_{X\text{-}ray}(T)$ parameters for the Eu(II) site at 203 K, the temperature of the single crystal X-ray data reported herein. The respective values are $F_{Möß}(203\ K)$ = 2.18(5) and $F_{X\text{-}ray}(203$ K) = 8.51(2), respectively (the latter was calculated from U_{ij} values observed in the single-crystal X-ray data). Clearly, what the X-ray value shows is much higher than would be expected on the basis of the Mößbauer data. In fact, the rather high value of $F_{X\text{-}ray}(203\ K)$ cannot reflect the $\langle x_{ave}{}^2\rangle$ values for the Eu atom since the recoil-free fraction would correspond to only 0.0127% and thus make the observation of the Mößbauer resonance unacceptably small. It is therefore reasonable to assume that the disagreement of the two F parameters arises

dx.doi.org/10.1021/ic4028546 | Inorg. Chem. 2014, 53, 2188−2194

either from static disorder or is due to low-frequency librational and torsional modes, which influence the X-ray data, but to which the Mößbauer measurements are insensitive. This means that the metal in the europocene Cp^{BIG}_2Eu is statistically disordered over several positions on a plane parallel to the Cp planes and that the nature of this disorder is static rather than dynamic. Thus, the proposed structure in which the Eu atom is slightly off-center (Scheme 1d) can be regarded as a truly bent structure. The large anisotropy found in the crystal structure is caused by different directions of off-center slippage throughout the crystal. Whereas the Mößbauer technique is insensitive to this static disorder, the X-ray methodology is sensitive to this effect.

Despite the parallel Cp^{BIG} planes in Cp^{BIG}_2M, metallocenes with heavier alkaline-earth and lanthanide(II) metals can therefore be considered as bent complexes in which the angle $Cp_{center}-M-Cp_{center} < 180°$. The off-center slippage (or nonlinearity) in these complexes increases with metal size: Ca < Sr < Ba. In contrast to expectation, the lanthanides show more extreme disorder and therefore more bending than the group 2 metals. Note that Sm^{2+}, Eu^{2+}, and Sr^{2+} are of similar size (Table 1) and usually give identical crystal structures with surprisingly similar bond distances and angles. Similarly, crystal structures of Yb^{2+} complexes can be compared to those of equisized Ca^{2+}.[32]

Although the distances in the Cp^{BIG}_2M metallocenes for the Yb/Ca and Sr/Eu(or Sm) couples are remarkably similar, the extent of metal atom disorder differs significantly. These differences can be explained by assuming that metal polarization is responsible for this type of disorder. Bonding in these metallocenes is predominantly ionic, and off-center slippage of the 2+ cation leads to polarization of this nucleus by the field of the negatively charged Cp^{BIG} anions (Scheme 1d).

Table 1 includes the calculated static electric dipole polarizabilities for the M^{2+} ions at the second-order Douglas–Kroll coupled-cluster level, DK2-CCSD(T). The dipole polarizabilities for Ca^{2+}, Sr^{2+}, Ba^{2+}, and Sn^{2+} at this rather accurate level of theory are known in the literature,[33,34] whereas those for the lanthanide(II) ions Sm^{2+}, Eu^{2+}, and Yb^{2+} were currently unknown, except from early Hartree–Fock estimates.[35] For an accurate comparison of dipole polarizabilities, we therefore decided to calculate those for Sm^{2+}, Eu^{2+}, and Yb^{2+} at the same high level (details can be found in the Experimental Section). For the group 2 metal cations the polarizability increases with atomic number ($Ca^{2+} < Sr^{2+} < Ba^{2+}$) as does the metal atom disorder and thus $Cp_{center}-M-Cp_{center}$ bending. In contrast, for the lanthanide(II) cations the polarizability decreases with atomic number ($Sm^{2+} > Eu^{2+} > Yb^{2+}$) due to the fact that the ion size decreases on account of the well-known lanthanide contraction. (A similar trend is found for the neutral lanthanide and actinide atoms.)[36] The trend in polarizability for the cations fits with the decrease of metal disorder along the row $Sm^{2+} \approx Eu^{2+} > Yb^{2+}$.

Of particular notice is the comparison between the alkaline-earth/lanthanide couples: Ca/Yb and Sr/Sm or Sr/Eu. The polarizabilities of the lanthanide(II) cations are larger than those of their equisized group 2 metal cations, likely on the basis of the (partially) filled f shell. This explains why the disorder for Yb is similar to that found for Sr and not comparable to that of Ca. It also shows why disorder for Sm and Eu is larger than that found for Sr. Apart from Ba^{2+}, which has the highest polarizability but not the most extreme metal disorder, the results seem again to be consistent. Therefore, taking a metal polarizability as an argument for metallocene bending could explain metal disorder in Cp^{BIG}_2M sandwich complexes with parallel Cp rings.

The stannocene Cp^{BIG}_2Sn shows no metal-atom disorder and should be considered as a metallocene with a truly linear $Cp_{center}-Sn-Cp_{center}$ geometry. This seems in striking contrast with the rather large polarizability of the Sn^{2+} ion (Table 1). However, bonding between C and the late main-group metal Sn is predominantly covalent, and a polarization model in which negatively charged Cp rings polarize the central metal is not valid. Consequently an ordered, truly linear structure is found. Moreover, for the group 2 metals not only the core polarizability becomes important for the bending behavior[9a] but also the mixing with the low-lying unoccupied d orbitals. For Sn^{2+} there are no low-lying d orbitals available.

CONCLUSIONS

Comparing the crystal structures of Cp^{BIG}_2Sn with those of other Cp^{BIG}_2M metallocenes (M = Ca, Sr, Ba, Sm, Eu, Yb) shows that the stannocene features all typical characteristics for this compound class: perfect linearity, C–H···C(π) bonding between the Cp^{BIG} rings, and out-of-plane bending of the aryl substituents toward the metal. There is, however, a striking difference in the displacement parameters for the metal atoms. The stannocene shows a perfectly ordered metal atom with small displacement factors and anisotropy (as expected for a heavy metal atom); whereas, the metals in the other metallocenes show large displacement factors in a plane parallel to the rings. Although this would suggest that the alkaline-earth and lanthanide(II) metals are more dynamic than Sn(II), a comparison of ^{151}Eu and ^{119}Sn Mößbauer investigations shows the opposite. In the temperature range of ca. 100–250 K the metal atom vibrational amplitudes are larger for Sn(II) than they are for Eu(II), as is expected on account of their different atomic weights. Thus, Eu in Cp^{BIG}_2Eu is more tightly bound than Sn in Cp^{BIG}_2Sn.

The large displacement factors in the group 2 and especially in the lanthanide(II) metallocenes Cp^{BIG}_2M can be explained by static metal disorder in a plane parallel to the Cp^{BIG} rings. Despite parallel Cp^{BIG} rings, these metallocenes can be considered as complexes with a nonlinear $Cp_{center}-M-Cp_{center}$ geometry. This nonlinearity can be explained by an ionic model in which metal atoms are polarized by the negatively charged Cp rings (Scheme 1d). The extent of nonlinearity is in line with trends found in M^{2+} ion polarizabilities. This model can not be applied to predominantly covalently bound Cp^{BIG}_2Sn, which shows a perfectly ordered structure. Therefore, the origin of bending in Cp^*_2M complexes should be revisited. For metallocenes with M = Ca, Sr, Ba, Sm, Eu, or Yb metal atom, polarizability is still an argument, as is van der Waals Cp*···Cp* attraction (the latter has been confirmed by recent calculations that show that dispersion effects indeed play a large role in such bent structures).[37] However, the bent geometry for Cp^*_2Sn should not be explained by metal polarizability (Scheme 1a) but is solely due to van der Waals Cp*···Cp* attraction (Scheme 1b) and is likely to some extent also influenced by a small p character component in the orbital on Sn containing the electron lone pair.

EXPERIMENTAL SECTION

All experiments were carried out under argon using standard Schlenk-techniques and freshly dried solvents. $Cp^{BIG}H$ has been prepared

dx.doi.org/10.1021/ic4028546 | Inorg. Chem. 2014, 53, 2188–2194

according to the literature.[38] NMR spectra were measured on a Bruker DPX300 spectrometer using predried deuterated solvents.

Synthesis of Cp^{BIG}_2Sn. The stannocene was prepared by in situ synthesis of $Cp^{BIG}Na$, which was reacted with $SnCl_2$. Addition of metallic sodium (19 mg, 0.83 mmol) to a solution of $Cp^{BIG}H$ (580 mg, 0.80 mmol) in 40 mL of toluene resulted in slow formation of hydrogen gas. The solution was heated overnight to 110 °C. After it was cooled, the solvent was removed, and the product was dried under high vacuum. This gave $Cp^{BIG}Na$ as a yellow-orange powder in quantitative yield (600 mg, 0.80 mmol). A mixture of 600 mg (0.80 mmol) of $Cp^{BIG}Na$ and 76 mg of (0.40 mmol) $SnCl_2$ in 5 mL of THF was stirred for 4 d at room temperature. The white precipitate was removed by centrifugation to give a yellow solution. All volatiles were removed, and the yellow residue was dissolved in a 2:1 mixture of warm hexane and THF. Cooling the solution to −20 °C gave the crystal-pure product Cp^{BIG}_2Sn as large yellow block-like crystals. Yield: 233 mg (0.15 mmol, 37%). Anal. Calcd for $C_{110}H_{130}Sn$: C, 84.09; H, 8.35. Found: C, 83.06; H, 8.11%. ^{1}H NMR (300 MHz, benzene-d_6, 25 °C): δ = 0.97 (t, $^3J_{(H,H)}$ = 6.9 Hz, 30H, $CH_2CH_2CH_2CH_3$), 1.36 (m, $^3J_{(H,H)}$ = 6.9 Hz, 20H, $CH_2CH_2CH_2CH_3$), 1.57 (m, $^3J_{(H,H)}$ = 6.9 Hz, 20H, $CH_2CH_2CH_2CH_3$), 2.52 (t, $^3J_{(H,H)}$ = 6.9 Hz, 20H, CH_2CH_2-CH_2CH_3), 6.91 (d, $^3J_{(H,H)}$ = 6.0 Hz, 20H, CH_{arom}), 7.31 (d, $^3J_{(H,H)}$ = 6.0 Hz, 20H, CH_{arom}). ^{13}C NMR (300 MHz, benzene-d_6, 25 °C): δ = 14.22 ($CH_2CH_2CH_2CH_3$), 22.76 ($CH_2CH_2CH_2CH_3$), 34.14 ($CH_2CH_2CH_2CH_3$), 35.76 ($CH_2CH_2CH_2CH_3$), 126.83 (C_{arom}), 127.96 (C_{arom}), 133.53 (C_{arom}), 133.05 (C_{arom}), 140.65 (C_{arom}). ^{119}Sn-NMR (300 MHz, benzene-d_6, 25 °C): δ = −2190.

Crystal Structure Determination of Cp^{BIG}_2Sn. Data were collected on a Siemens SMART CCD diffractometer with Mo Kα radiation (0.71073 Å) and an APEX II detector. Intensities were corrected for absorption using the semiempirical psi-scan method. Crystal structures have been solved by direct methods (SHELXS-97)[39] and were refined with SHELXL-97.[40] All geometry calculations and graphics have been performed with PLATON.[41]

Measurement at 203 K (Mo Kα), formula $C_{110}H_{130}Sn$, triclinic, a = 13.1315(12) Å, b = 14.0227(7) Å, c = 14.3112(6) Å, α = 117.096(2)°, β = 98.514(3)°, γ = 94.010(3)°, V = 2291.8(3) Å^3, space group $P\bar{1}$, Z = 1, ρ_{calc} = 1.138 g cm^{-3}, μ(Mo Kα) = 0.325 mm^{-1}, 30 258 measured reflections, 10 196 independent reflections (R_{int} = 0.035), 9190 reflections observed with $I > 2\sigma(I)$, θ_{max} = 27.6°, R = 0.0382, $wR2$ = 0.0932, GOF = 1.02, 587 parameter, min/max residual electron density −0.37/+0.54 e Å^{-3}. The aromatic hydrogen atoms were located in the difference Fourier map and were refined isotropically. All other hydrogen atoms have been placed on ideal calculated positions and were refined in a riding mode.

CCDC 965200 contains the supplementary crystallographic data for this paper. These data can be obtained free of charge from the Cambridge Crystallographic Data Centre via www.ccdc.cam.uk/data_request.cif.

Mößbauer Spectroscopy. The sample was received in a closed Schlenk tube under nitrogen, which was opened in an inert atmosphere glovebox and transferred to O-ring Perspex sample holders, which were then immediately cooled to 78 K in liquid nitrogen. Temperature-dependent Mössbauer effect spectroscopy was effected in transmission geometry employing a $CaSnO_3$ source for the tin measurements and a $^{151}Sm_2O_3$ source for the Eu measurements. The isomer shifts of the former are referred to a $BaSnO_3$ room-temperature absorber spectrum, and the latter to a EuF_3 room-temperature absorber spectrum. Temperature monitoring was effected using the Daswin software,[42] and temperature stability was better than ±1 K over the data acquisition intervals. Velocity calibration of the spectrometer was effected using a 20 mg/cm^2 α-Fe absorber at room temperature.

Static Dipole Polarizability Calculations. The dipole polarizabilities for the ^{7}F state of Sm^{2+} ($4f^6$), the ^{8}S state of Eu^{2+} ($4f^7$), and the ^{1}S state of Yb^{2+} ($4f^{14}$) have been calculated using a finite field method with homogeneous electric field perturbations of 0, 0.001, and 0.002 au within a second-order Douglas-Kroll (DK) relativistic treatment[43] together with coupled-cluster singles-doubles and perturbative triples to account for electron correlation.[34,44] Both relativistic and electron correlation effects are important for the lanthanides and need to be included, that is, at the Hartree−Fock level the polarizabilities increase due to scalar relativistic effects by 0.43 au for Sm^{2+}, by 0.28 au for Eu^{2+}, and by 0.27 au for Yb^{2+}, and electron-correlation effects (at the DK-CCSD(T) level of theory), which are of equal importantance, increase the polarizability by 1.12 au for Sm^{2+}, by 0.83 au for Eu^{2+}, and by 0.44 au for Yb^{2+} at the scalar relativistic level of theory. Contracted segmented (24s,17p,13d,7f,5g)/(19s,13p,10d,4f,3g) basis sets with augmented diffuse functions were used for the lanthanides,[45] resulting in 403 contracted to 163 basis functions. The basis set was tested for stability with respect to the electric field perturbation. The rather large polarizability of closed-shell Sn^{2+} (^{1}S) of 15.15 au published by Kellö et al.[46] differs somewhat from the Fraga et al.'s estimated value of 18.2 au. We therefore reinvestigated the polarizability of Sn^{2+} using a much improved uncontracted and extended (35s,28p,20d,4f,1g) Dyall basis set.[47] Our calculated DK-CCSD(T) polarizability of 15.32 au is in good agreement with Kellö's original result. Here scalar relativistic effects lower the polarizability by 2.90 au at the Hartree−Fock level because of the large relativistic contraction of the Sn(5s) orbital. Electron correlation effects are also important, lowering the polarizability by 2.58 au at the DK level of theory. The rather large polarizability of Sn^{2+}, in contrast to the group 2 cations, is rather well explained through the sum-overstates (oscillator strength) formula and the energetically low-lying unoccupied 5p orbitals in Sn^{2+}. For example, the Sn^{2+} excitation from $5s^2 \rightarrow 5s^1p^1$ ($^1S \rightarrow {}^1P$) is at 9.91 eV in comparison to the $3p^6 \rightarrow 3p^5 4s^1$ ($^1S \rightarrow {}^1P$) transition of Ca^{2+}, which comes at 30.71 eV.

AUTHOR INFORMATION

Corresponding Author

*E-mail: sjoerd.harder@fau.de. (S.H.) Fax: 49-9131-8527387. E-mail: HERBER@VMS.HUJI.AC.IL. (R.H.H.) Fax: 972-2-6586347.

Notes

The authors declare no competing financial interest.

ACKNOWLEDGMENTS

We thank Prof. Dr. R. Boese and D. Bläser for collection of the X-ray data and acknowledge the DFG for financial support.

REFERENCES

(1) Evans, W. J.; Hughes, L. A.; Hanusa, T. P. *J. Am. Chem. Soc.* **1984**, *106*, 4270.

(2) Evans, W. J.; Hughes, L. A.; Hanusa, T. P.; Doedens, R. J. *Organometallics* **1986**, *5*, 1285.

(3) Andersen, R. A.; Boncella, J. M.; Burns, C. J.; Blom, R.; Haaland, A.; Volden, H. V. *J. Organomet. Chem.* **1986**, *312*, C49.

(4) (a) Andersen, R. A.; Blom, R.; Burns, C. J.; Volden, H. V. *J. Chem. Soc., Chem. Commun.* **1987**, 768. (b) Andersen, R. A.; Blom, R.; Boncella, J. M.; Burns, C. J.; Volden, H. V. *Acta Chem. Scand.* **1987**, *A41*, 24.

(5) Williams, R. A.; Hanusa, T. P.; Huffman, J. C. *Organometallics* **1990**, *9*, 1128.

(6) Kaupp, M.; Schleyer, P. v. R.; Dolg, M.; Stoll, H. *J. Am. Chem. Soc.* **1992**, *114*, 8202.

(7) Hollis, T. K.; Burdett, J. K.; Bosnich, B. *Organometallics* **1993**, *12*, 3385.

(8) Burkey, D. J.; Hanusa, T. P. *Comments Inorg. Chem.* **1995**, *17*, 41.

(9) (a) Szentpaly, L. v.; Schwerdtfeger, P. *Chem. Phys. Lett.* **1990**, *170*, 555. (b) Kaupp, M.; Schleyer, P. v. R.; Stoll, H.; Preuss, H. *J. Chem. Phys.* **1991**, *94*, 1360.

(10) Jutzi, P.; Burford, N. *Chem. Rev.* **1999**, *99*, 969.

(11) Schultz, M.; Burns, C. J.; Schwartz, D. J.; Andersen, R. A. *Organometallics* **2000**, *19*, 781.

(12) Kaupp, M. *Angew. Chem., Int. Ed.* **2001**, *40*, 3535.

(13) Hanusa, T. P. *Organometallics* **2002**, *21*, 2559.

(14) Kaupp, M.; Charkin, O. P.; Schleyer, P. v. R. *Organometallics* **1992**, *11*, 2765.
(15) Dory, T. S.; Zuckerman, J. J. *J. Organomet. Chem.* **1984**, *264*, 295.
(16) (a) Dory, T. S.; Zuckerman, J. J.; Barnes, C. L. *J. Organomet. Chem.* **1985**, *281*, C1. (b) Hani, R.; Geanangel, R. A. *J. Organomet. Chem.* **1985**, *293*, 197.
(17) Harvey, M. J.; Quisenberry, K. T.; Hanusa, T. P.; Young, V. G., Jr. *Eur. J. Inorg. Chem.* **2003**, 3383.
(18) Sitzmann, H.; Dezember, T.; Schmitt, O.; Weber, F.; Wolmershauser, G. *Z. Anorg. Allg. Chem.* **2000**, *626*, 2241.
(19) Heeg, M. J.; Janiak, C.; Zuckerman, J. J. *J. Am. Chem. Soc.* **1984**, *106*, 4259.
(20) Deacon, G. B.; Forsyth, C. M.; Jaroschik, F.; Junk, P. C.; Kay, D. L.; Maschmeyer, T.; Masters, A. F.; Wang, J.; Fields, L. D. *Organometallics* **2008**, *27*, 4772−4778.
(21) Janiak, C.; Schumann, H.; Stader, C.; Wrackmeyer, B.; Zuckerman, J. J. *Ber. Bunsen-Ges.* **1988**, *121*, 1745.
(22) Koelle, U.; Khouzami, F. *Angew. Chem., Int. Ed. Engl.* **1980**, *19*, 640.
(23) Broadley, K.; Lane, G. A; Connelly, N. G.; Geiger, W. E. *J. Am. Chem. Soc.* **1983**, *105*, 2486.
(24) Kuchenbecker, D.; Harder, S.; Jansen, G. *Z. Anorg. Allg. Chem.* **2010**, *636*, 2257.
(25) Orzechowski, L.; Piesik, D. F.-J.; Ruspic, C.; Harder, S. *Dalton Trans.* **2008**, 4742.
(26) Ruspic, C.; Moss, J. R.; Schürmann, M.; Harder, S. *Angew. Chem., Int. Ed.* **2008**, *47*, 2121.
(27) Harder, S.; Naglav, D.; Ruspic, C.; Wickleder, C.; Adlung, M.; Hermes, W.; Eul, M.; Pöttgen, R.; Rego, D. B.; Poineau, F.; Czerwinski, K. R.; Herber, R. H.; Nowik, I. *Chem. Eur. J.* **2013**, *19*, 12272.
(28) (a) Shannon, R. D. *Acta Crystallogr.* **1976**, *A32*, 751. (b) Shannon, R. D.; Prewitt, C. T. *Acta Crystallogr.* **1969**, *B25*, 925. (c) Shannon, R. D.; Prewitt, C. T. *Acta Crystallogr.* **1970**, *B26*, 1046.
(29) Williamson, R. L.; Hall, M. B. *Organometallics* **1986**, *5*, 2142.
(30) Heeg, M. J.; Herber, R. H.; Janiak, C.; Zuckerman, J. J.; Schumann, H.; Manders, W. F. *J. Organomet. Chem.* **1988**, *346*, 321.
(31) (a) Herber, R. H.; Nowik, I. *J. Nucl. Radiochem. Sci.* **2008**, *2*, 33. (b) Herber, R. H.; Nowik, I. *J. Organomet. Chem.* **2008**, *693*, 3007. (c) Herber, R. H. *J. Organomet. Chem.* **2012**, *717*, 41 and references therein..
(32) Harder, S. *Angew. Chem., Int. Ed.* **2004**, *43*, 2714.
(33) The following website gives a useful overview: http://ctcp.massey.ac.nz/dipole-polarizabilities (accessed November 1, 2013).
(34) Lim, I.; Schwerdtfeger, P. *Phys. Rev. A* **2004**, *70*, 062501.
(35) Fraga, S.; Karwowski, J.; Saxena, K. M. S. *At. Data Nucl. Data Tables* **1973**, *12*, 467.
(36) Thierfelder, C.; Schwerdtfeger, P. *Phys. Rev. A* **2009**, *79*, 032512.
(37) Labouille, S.; Clavaguéra, C.; Nief, F. *Organometallics* **2013**, *32*, 1265.
(38) Dyker, G.; Heiermann, J.; Miura, M.; Inoh, J. I.; Pivsa-Art, S.; Satoh, T.; Nomura, M. *Chem.—Eur. J.* **2000**, *6*, 3426.
(39) Sheldrick, G. M. SHELXS-97, *Program for Crystal Structure Solution*, Universität Göttingen: Germany, 1997.
(40) Sheldrick, G. M. SHELXL-97, *Program for Crystal Structure Refinement*, Universität Göttingen: Germany, 1997.
(41) Spek, A. L. PLATON, *A Multipurpose Crystallographic Tool*, Utrecht University: Utrecht, The Netherlands, 2000.
(42) Daswin software: Glaberson, private communication. Free software http://megadaq.com.
(43) (a) Douglas, M.; Kroll, N. M. *Ann. Phys. (N.Y.)* **1974**, *82*, 89. (b) Hess, B. A. *Phys. Rev. A* **1986**, *33*, 3742.
(44) Frisch, M. J.; Trucks, G. W.; Schlegel, H. B.; Scuseria, G. E.; Robb, M. A.; Cheeseman, J. R.; Scalmani, G.; Barone, V.; Mennucci, B.; Petersson, G. A.; Nakatsuji, H.; Caricato, M.; Li, X.; Hratchian, H. P.; Izmaylov, A. F.; Bloino, J.; Zheng, G.; Sonnenberg, J. L.; Hada, M.; Ehara, M.; Toyota, K.; Fukuda, R.; Hasegawa, J.; Ishida, M.; Nakajima, T.; Honda, Y.; Kitao, O.; Nakai, H.; Vreven, T.; Montgomery, J. A.; , Jr., Peralta, J. E.; Ogliaro, F.; Bearpark, M.; Heyd, J. J.; Brothers, E.; Kudin, K. N.; Staroverov, V. N.; Kobayashi, R.; Normand, J.; Raghavachari, K.; Rendell, A.; Burant, J. C.; Iyengar, S. S.; Tomasi, J.; Cossi, M.; Rega, N.; Millam, J. M.; Klene, M.; Knox, J. E.; Cross, J. B.; Bakken, V.; Adamo, C.; Jaramillo, J.; Gomperts, R.; Stratmann, R. E.; Yazyev, O.; Austin, A. J.; Cammi, R.; Pomelli, C.; Ochterski, J. W.; Martin, R. L.; Morokuma, K.; Zakrzewski, V. G.; Voth, G. A.; Salvador, P.; Dannenberg, J. J.; Dapprich, S.; Daniels, A. D.; Ö. Farkas, Foresman, J. B.; Ortiz, J. V.; Cioslowski, J.; , and Fox, D. J., *Gaussian 09*, Revision D.01; Gaussian, Inc.: Wallingford, CT, 2009.
(45) Dolg, M. *J. Chem. Theory Comput.* **2011**, *7*, 3131.
(46) Kellö, V.; Antušek, A.; Urban, M. in Maroulis, G. *Computational Aspects of Electric Polarizability Calculations: Atoms, Molecules and Clusters;* IOS press: Amsterdam, 2006; p 519.
(47) Dyall, K. G. *Theor. Chem. Acc.* **2006**, *115*, 441.